ORDERLY THREE-DIMENSIONAL PROCESSES IN TURBULENT BOUNDARY LAYERS ON ABLATING BODIES

By Thomas N. Canning, Michael E. Tauber, Max E. Wilkins,
and Gary T. Chapman

Ames Research Center, NASA, Moffett Field, California, 94035, USA

1. INTRODUCTION

Careful experimental studies have revealed the presence of a remarkable degree of order in turbulent boundary layers. Two examples of this, which will also be cited as bases for the discussion of the present paper, are the work by Gregory and Walker (1) and by Mochizuki (2,3). These papers illustrate quite clearly that the wedge of turbulent flow produced by affixing a single element of roughness in a flat-plate boundary layer contains a highly regular system of longitudinal vortices which extend from the wedge leading edge to great distances downstream.

A number of studies have shown the existence of laterally spaced, time-variant disturbances in transitional subsonic and supersonic flows (4-8). More recently, the present authors (9,10) found what appeared to be regular markings on recovered ballistic-range cone models showing longitudinal as well as lateral periodicity, that is, a cross-hatching of the ablated surface, in addition to longitudinal vortices which ablated streamwise grooves in the surface. An example of this cross-hatching is shown in Fig. 1, taken from Ref. 10.

The possible implications of these crosshatched ablation patterns on the heat-shield performance of entry bodies have prompted the present study. This paper describes an attempt to link the observed sculpturing of the surfaces to the aerodynamic and thermodynamic test conditions under which they were produced.

2. FACILITIES AND TESTS

Most of the data and discussion will concern observations of Plexiglas models (polymethylmethacrylate), as affected by the hot hypersonic flow in the NASA Ames 3.5-foot wind tunnel. Where appropriate, comparison will be made with models recovered after flight in a ballistic range.

The 3.5-foot hypersonic wind tunnel is a blowdown facility, in which air stored at high pressure is heated as it passes upward through a cylindrical tank filled with hot zirconia pebbles. The hot air then passes through an axially symmetric, contoured nozzle ($M_\infty \doteq 7$), the walls of which are protected by a thin film of helium injected upstream of the nozzle throat. The tunnel exhausts into four evacuated spheres and can provide test times in excess of 1 minute at the conditions used in the present tests (stagnation pressure of 115 atm and stagnation temperatures of 750° and 1075° K).

The models were mounted on a movable sting, inserted into the test section after steady flow was established, and withdrawn after the desired test interval (before the flow was stopped). Insertion and withdrawal each required only a fraction of a second.

The models used in the experimental study were designed to reveal the influence of both gradual and abrupt, and positive and negative, pressure gradients on the patterns produced by ablation. Shapes were selected that would result in large pressure and heating-rate changes on a given model, along with large changes in boundary-layer-edge Mach number, M_E, (1.3 to 3.5) and unit Reynolds number (67,000 per cm to 640,000 per cm). The models (Fig. 2) were solid, homogeneous bodies of revolution (except for laminations) made of Plexiglas. Cone angles at the tip were 25°, 30°, 40°, and 50°; surface inclination was, in every case, changed by a 15° increment, which produced compressions on the two smaller tip angle cones, and expansions on those with larger tip angles. The slope was changed in two ways, discontinuously at a corner, and continuously on surfaces described by cubic equations. Pointed steel tips, about 1.2 cm in diameter, were used on the models to prevent ablation at the apex.

3. DATA

The data presented represent a detailed visual study of the bodies during and after testing. During the tests, the model surfaces were watched by one or more observers and were photographed by a 16 mm motion-picture camera at 128 frames per second. The observers' purpose was to determine the rate of formation of the surface patterns by the airflow and to signal the time for termination of the run by withdrawing the model. Since the plastic material is transparent and the surfaces appear frosted, many subtle details are better revealed by surface replicas than by the original surface. Two types of replica were made.

The more sensitive of the two consisted of epoxy plastic cast in a silicone-rubber mold made from the actual model. The rubber used adheres only weakly to the model and to the epoxy, and is easily separated with a small air jet. The rubber used for making the female impression is Dow Corning 3110 RTV Encapsulant, and the epoxy resin is Epocast Resin No. 4-L with hardener No. 9111. In the course of making these replicas it was found desirable to provide hollow liners in order to save rubber and epoxy material and make the final bodies light. Liners were made by vacuum-forming clear-plastic sheets of 0.508 mm to 1.270 mm thickness over the models. A rather high degree of detail was replicated in both of these processes, and many features difficult or impossible to see

and photograph on the actual models are made easily visible. Photographs of all of the epoxy replicas are shown in Fig. 3. There are more replicas than models since two models were tested twice in the wind tunnel and replicas were made after each test.*

Several techniques were used to measure dimensions and angles of surface patterns from the models and replicas. One very sensitive process was to make pencil rubbings by pressing a piece of bond paper tightly against the model or replica surface and stroking lightly with the side of a lead pencil or a soft, colored pencil. Both longitudinal and lateral strokings were used to get best results. The features were then identified and measured in the flat.

On very subtly sculpted models (Fig. 3(e)) or deeply ablated models (Fig. 3(f)), it was found desirable to hand-mark the features with a grease pencil while studying them with different lighting and viewing angles. After the principal features were thus accentuated, the pencil marks could be either "transferred" using pressure-sensitive tape (and transported to flat paper as in the case of rubbings) or measured in place. Some features, however, were so clearly marked that there was no difficulty in measuring them directly.

In order to minimize any personal bias in the measurement of pattern sizes and shapes, two of the authors made totally independent measurements of the sweep angle and longitudinal and lateral wavelengths of the crosshatch patterns at positions on the bodies selected by each for clarity of markings. Several measurements were made in each region so that the results would have some statistical value, but no averaging has been done in the data presentation. The results of the independent studies were substantially identical.

3.1. Appearance of Ablated Surfaces

After ablation by the hypersonic test stream, the present models exhibited most of the features seen on the earlier ballistic-range models (9). For completeness of the present discussion these features are described briefly herein and related to those reported by other authors, as appropriate.

Each model had small regions of apparently uniform laminar flow, for at least a part of the test time, which produced little in the way of surface sculpting. These regions usually ended at a highly irregular transition front characterized by roughness elements and their resultant more deeply eroded "wedges." The wedges appear similar in planform to those observed in Refs. 1-3, 9, and 10. Their lateral rate of growth is similar as is the occasionally observed longitudinal grooving inside them.**

The most striking feature in the turbulent wedges and elsewhere in the regions of presumably turbulent flow is the cross-hatching produced by the flow. That the patterns result from intersecting grooves which spiral in both directions around the bodies is clearly evident from the slightly ablated bodies (Fig. 3(e)). As the ablation proceeds, the grooves appear to influence the nature of the adjacent flow more and more strongly. Instead of clearly intersecting, the grooves appear to join longitudinally at the spiral intersections and produce a set of wavy longitudinal grooves like those shown in Fig. 3(f) on model 4.

The clarity and depth of the crosshatch patterns is occasionally enhanced by disturbances produced by flaws or joints in the models as seen in Fig. 3(d). A cursory examination showed that new grooves were being created more or less continuously along the surfaces so that the spacing did not increase proportionately with body radius.

3.2. Correlations

In general, the sculpture produced by ablation is seen to be quite complicated, and our first effort at relating the forms produced to the test conditions is necessarily limited. In the present case we have sought to correlate the spiral angle of the grooves, that is, the angle between the groove and the body-generator lines, and the size of the patterns with the boundary-layer-edge flow conditions.

3.2.1. Spiral Angle Correlation

Although the influence of material properties has not been ruled out, it was postulated at the outset that the surface patterns were governed by the boundary layer and perhaps the exterior flow. Accordingly, the spiral angle data for all the models were plotted against the boundary-layer-edge Mach number to obtain Fig. 4. A rather convincing correlation is seen between the observed spiral angle and the Mach angle. If the spiral is established by a standing wave, it must of necessity be at a greater angle than the Mach angle at the boundary-layer edge. The quality of the correlation suggests that a standing wave system does in fact exist, and hence that the cross-hatching should

*In general, the replicas do not extend fully to the base of the original model. For the purpose of making the replicas only, in some cases the steel tip was removed from the model nose and replaced with a screw. The apparent blunting of model tips, such as in Fig. 3(c), was caused by air trapped during casting and does not represent the actual condition of the model during the test.

**The bodies also exhibited, in varying degrees, two other types of markings. One consisted of very fine scale longitudinal ridges along body generators (see Fig. 3(h)); these may be a product of small longitudinal vortices. The other markings are small surface craters partly surrounded by crescents immediately downstream of each crater (see Fig. 3(c)); these are thought to be produced by the impact of zircona dust particles present in the test stream.

not exist in subsonic flow. Mateer and Larson (11) conducted a test series using cones of various materials and a range of apex angles in the same facility and found cross-hatching only on bodies with supersonic flow outside the boundary layer. The points above the Mach angle curve suggest that the disturbance source of the standing wave can be well inside the boundary layer where the Mach numbers are lower than M_e. One level in the boundary layer which might be critical is that at which temperature is maximum.

3.2.2. Lateral-Spacing Correlation

Since the shape of the pattern, that is, the spiral angle, is related to the flow properties, a length was sought to which the size of the pattern (longitudinal or lateral spacing of grooves) could be satisfactorily related. Several lengths were considered: the various boundary-layer thicknesses, the distance from the surface to the shock wave, the wetted length along the surface from the apex, the radius of curvature of the surface, and the depth of melted surface material, if any. In addition to these lengths, the influence of such factors as absolute heating rate and Mach number on pattern size was checked as well.

Even a cursory examination of the models showed a wide variation of groove spacing at any particular body station. New grooves continuously appear as the flow stretches around the expanding body; this means that the minimum groove spacing is, at the very greatest, half the maximum. Also, since there are doubtless random influences affecting groove initiation, the ratio of maximum spacing to minimum must exceed 2. At a particular streamwise location on model 4 a groove variation of fourfold over the minimum was observed. In view of these variations, only an approximate characterization was possible with the data available.† No obvious effect of the pressure gradient on such features as the cross-hatching has been found; however, because of the influence of the pressure on the heat-transfer rate, significant changes occurred in the depth of the surface markings.

Many dimensionless groupings were attempted in the course of studying these data and almost all appeared to yield substantially poorer correlation than that given by a Reynolds number based on boundary-layer-edge conditions and the lateral spacing between the oblique grooves, Re_{λ_y}, plotted as a function of the Reynolds number based on local thickness of the turbulent boundary layer, Re_δ. The correlation showed that Re_{λ_y} increased with Re_δ (Fig. 5). This finding has two weaknesses: first, it is based on one test of model 3 at higher total temperature (filled symbols). Second, in two-dimensional flow it would be necessary for grooves to disappear selectively in order to permit the spacing to increase so as to avoid passing out of the correlation band. Mateer and Larson found no such selective disappearance in tests with plastic wedges. An alternative to selective disappearance might be that the entire periodic system might simply decay generally and produce imperceptible ablation patterns. In view of the slow decay of longitudinally disposed vortices this might require great distances.

A few measurements of λ_y were made on the ballistic-range models of Ref. 9. Since there is little chance of accurately determining when during the flights the final patterns formed, accurate calculations of Re_{λ_y} and Re_δ are not possible. The complications added by the possibility of sizable mass transfer at the surface add to the difficulty of interpretation. Roughly, the values of Re_{λ_y} fell near the bottom of the scatter band in Fig. 5.

The present findings together with those of earlier experiments (clearly defined laterally periodic structure in turbulent boundary-layer flows) lead to a possible model for the inception of cross-hatching and other sculpture of ablated surfaces.

4. POSTULATED MODEL

The flow processes in the boundary layer, which are thought to be capable of sculpting the present patterns (and some other patterns observed earlier as well), are described without qualifying remarks in this section. Subsequently, supporting observations taken from the present experiments and from the literature are presented to lend weight to the description.

4.1. Postulated Flow

The establishment of a turbulence wedge, such as diagrammed in Fig. 6, starts with a single-disturbance source a (e.g., a roughness element) in a laminar boundary layer b. The trailing vortex system c from the disturbance may be steady downstream for a distance, depending on such factors as disturbance size and flow Reynolds number, and then suddenly break down into intense oscillation and turbulence at d in Fig. 6. The disturbance generated by this breakdown produces a nearly perfectly symmetrical spreading pattern of turbulent flow containing a regular array of discrete longitudinal vortices e, which are formed at the wedge leading edge. The disturbance f along the leading edge either produces or is produced by a vortex roughly hyperbolic in form near

†Near the beginning of the test periods of some of the models a much smaller crosshatch pattern of waves was seen in the thin melt layer. The spiral angle of these wavelets appeared to be the same as that of the grooves produced later, but the spacing of the waves was perhaps smaller by a factor of 3 or 4 than the final markings. They may be like the line cross-hatching shown in Ref. 10. Their smaller size and impermanence suggest that some change in material response, such as temporary development of melt layers of critical thickness, surface tension, or viscosity, may have an important influence on wave spacing in either the small temporary or large permanent patterns observed.

its apex. The longitudinal vortex filaments are regularly spaced. The pressure disturbance resulting from the formation of each filament propagates within the Mach cone g, as indicated in Fig. 6. The array of pressure pulses can excite oscillations in the boundary layer as might a multitude of randomly spaced disturbances in view of the potential for self-aggravation (i.e., feedback) and stabilization introduced by the sculptured pattern. These disturbances do not produce noticeable local increases in heat transfer or ablation outside the wedge h where the flow is laminar; within the wedge, where the flow is turbulent, the wave-boundary-layer interaction is concentrated i and yields sharply defined increments in heating. Where the surface contouring by concentrated ablation becomes deep enough, the resulting disturbances become severe enough to supplant the hyperbolic-front vortex mechanism responsible for the earlier spread of turbulence, as shown at j, toward the rear of the sketched flow in Fig. 6. As the boundary layer stretches over the ever-expanding perimeter of the body, new three-dimensional elements (probably vortex pairs) are created and produce additional wave systems (and hence grooves).

4.2. Supporting Evidence

The observations of Gregory and Walker (1) and of Mochizuki (2,3) are examples indicating that the breakdown of the smooth trailing vortex system from a roughness element is hastened either by increasing the free-stream Reynolds number or the size of the roughness element. The suddenness of the breakdown is well documented (2). The disturbance generated by this breakdown is so strong and the resulting breakdown so regular that an almost perfectly symmetrical wedge is produced. Among the scores of turbulence wedges seen by the authors, no highly asymmetric turbulence wedges have ever been seen, so it is concluded that the ensuing spread of turbulence is fully controlled. That transition from laminar to turbulent flow, well known for uncertain behavior, should be so regular in this case attests to the dominance of this mechanism.

Both Refs. 1 and 2 note clearly the regular array of streamwise vortices found in the wedge. The extremely regular breakdown along the wedge leading edge is described in Ref. 3: ". . . the photographs of the smoke pattern show distinctly the turbulent region behind the sphere [roughness element] and the laminar region outside of it. At the boundary of the two regions, we can see the smoke filaments gather one after another and take winded forms and then become obscure by strong mixing downstream. This state indicates that there might be a longitudinal vortex near the boundary. The measurements of the mean velocity profiles show clearly that a pair of longitudinal vortices appears outside of the four longitudinal vortices existing already, just at the boundaries of the turbulence wedge, and much closer to the flat plate than the former vortices." The indication that all of these outer vortices (in each half of the wedge) are co-rotational also suggests that the mechanism controlling filament formation is not simple induction by the downwash fields of existing vortices, but is the result of a continuous vortex filament or a pressure wave passing obliquely across the flow.

An unusual observation on recovered ballistic-range models (9,10) may be further evidence of this postulated leading-edge vortex. The surface shown in Fig. 7(a) has a clearly visible low ridge called a "hyperbolic front" by the authors; several such fronts have been preserved on ballistic-range models. If the leading-edge vortex described in Ref. 3 does exist, it should induce a lateral flow near the surface such that the surface streamline will trace out a line following the ridge found. The flow detail here is suggested at f in Fig. 6.

The pressure disturbances produced by the start of each vortex filament forming at this front should produce sharp pulses propagating along the Mach cones from each formation point. In subsonic flow no such obvious mechanism exists for concentrating the effect of the pulses, and cross-hatching is not observed. Also, a convincing correlation is found between spiral angle and edge Mach number.

In a laminar boundary layer h (i.e., along the outbound waves, g), the streamwise action of each wave should be spread out over many boundary-layer thicknesses, perhaps over several wave spaces, because of the extensive interaction typical of waves with laminar boundary layers, and therefore produce no important sculpture unless it is strong enough by itself to cause transition (j in Fig. 6), as illustrated in Fig. 7(b). The inward-bound waves, g, on the other hand, are interacting with a boundary layer of much higher shear, so that the interaction is concentrated sharply. This should permit the cutting of grooves in the turbulent-flow area. As the flow is stretched over the body, new grooves appear. That the lateral wavelength does not exceed some poorly defined maximum probably related to the boundary-layer thickness is shown by the present data. The observations using hydrogen-bubble flow visualization in two-dimensional flow (7) show that even at very large Reynolds numbers there is a clear lateral periodicity in turbulent-boundary-layer profiles. Consistent with the results of Ref. 7, Black's analytical formulation (12) points strongly to the possibility of vortex-loop discharges into the outer part of the layer from near the surface at preferred lateral spacings.

This overall flow model for the initiation and development of turbulence and cross-hatching is believed to reconcile many of the observed phenomena in transitional and turbulent flow. The high degree of order found is consistent with the orderliness of the markings.

5. CONCLUDING REMARKS

It has been shown herein that there can be a great deal of order in the supersonic turbulent boundary layer. The presence of both lateral and longitudinal, nearly time-invariant, spatially fixed waves or vortex systems or both has been deduced from studying ablated surfaces under widely varying test conditions, ranging from those of ballistic ranges to wind tunnels. The sizes of the

models ranged over an order of magnitude, while surface pressures and heat-transfer rates varied over two to three orders of magnitude. The generally good agreement of "crosshatch" spiral angle with the boundary-layer-edge Mach angle up to about $M_e = 2$ and then spreading, at times, at an angle greater than the Mach angle, suggests that the disturbance causing the standing-wave system responsible can be near the edge or deeper within the boundary layer as Mach number increases. The attempt to correlate the spacing of the cross-hatching against a boundary-layer thickness has been only partially successful; typically, the wavelength is equal to a few boundary-layer thicknesses. Lastly, the model proposed herein for the formation of the cross-hatching is felt to be compatible with many of the critical elements of orderly flow found by earlier investigators.

ACKNOWLEDGMENT

The authors would like to acknowledge the contribution of Mr. Hartmut Legner in designing the models and doing many of the flow-field calculations.

6. REFERENCES

1. Gregory, N.; and Walker, W. S.: "The Effect on Transition of Isolated Surface Excrescences in the Boundary Layer." Part I, R. & M. No. 2779, Aeronautical Research Council, London, October 1956.

2. Mochizuki, Masako: "Smoke Observation on Boundary Layer Transition Caused by a Spherical Roughness Element." J. Physical Society of Japan, vol. 16, no. 5, May 1961, pp. 995-1008.

3. Mochizuki, Masako: "Hot-Wire Investigations of Smoke Patterns Caused by a Spherical Roughness Element." Natural Science Report, vol. 12, no. 2, Ochanomizu University, Tokyo, Japan, 1961.

4. Hama, Francis R.: "Some Transition Patterns in Axisymmetric Boundary Layers." Physics of Fluids, vol. 2, no. 6, November-December 1959, pp. 664-667.

5. Hama, Francis R.; and Nutant, John: "Detailed Flow-Field Observations in the Transition Process in a Thick Boundary Layer." Proceedings of the 1963 Heat Transfer and Fluid Mechanics Institute (Stanford University Press, Stanford, California, 1963), pp. 77-93.

6. Coles, Donald: "Transition in Circular Couette Flow." J. Fluid Mechanics, vol. 21, part 3, March 1965, pp. 385-425.

7. Schraub, F. A.; Kline, S. J.; Henry, J.; Runstadler, P. W., Jr.; and Littell, A.: "Use of Hydrogen Bubbles for Quantitative Determination of Time Dependent Velocity Fields in Low Speed Water Flows." Report MD-10, Stanford University, Stanford, California (February 1964).

8. Knapp, C. F.; and Roache, P. J.: "A Combined Visual and Hot-Wire Anemometer Investigation of Boundary-Layer Transition." AIAA J., vol. 6, no. 1, January 1968, pp. 29-36.

9. Canning, Thomas N.; Wilkins, Max E.; and Tauber, Michael E.: "Boundary-Layer Phenomena Observed on the Ablated Surfaces of Cones Recovered After Flights at Speeds Up to 7 km/sec." Presented at AGARD Specialists' Meeting on Fluid Physics of Hypersonic Wakes, Fort Collins, Colorado, May 10-12, 1967.

10. Canning, Thomas N.; Wilkins, Max E.; and Tauber, Michael E.: "Ablation Patterns on Cones Having Laminar and Turbulent Flows." AIAA J., vol. 6, no. 1, 1968, pp. 174-175.

11. Mateer, George G.; and Larson, Howard K.: "Unusual Boundary-Layer Transition Results on Cones in Hypersonic Flow." AIAA Preprint 68-40, 1968.

12. Black, Thomas J.: "Some Practical Applications of a New Theory of Wall Turbulence." Proceedings of the 1966 Heat Transfer and Fluid Mechanics Institute, edited by M. A. Saad and J. A. Miller (Stanford University Press, Stanford, California, 1966), pp. 366-386.

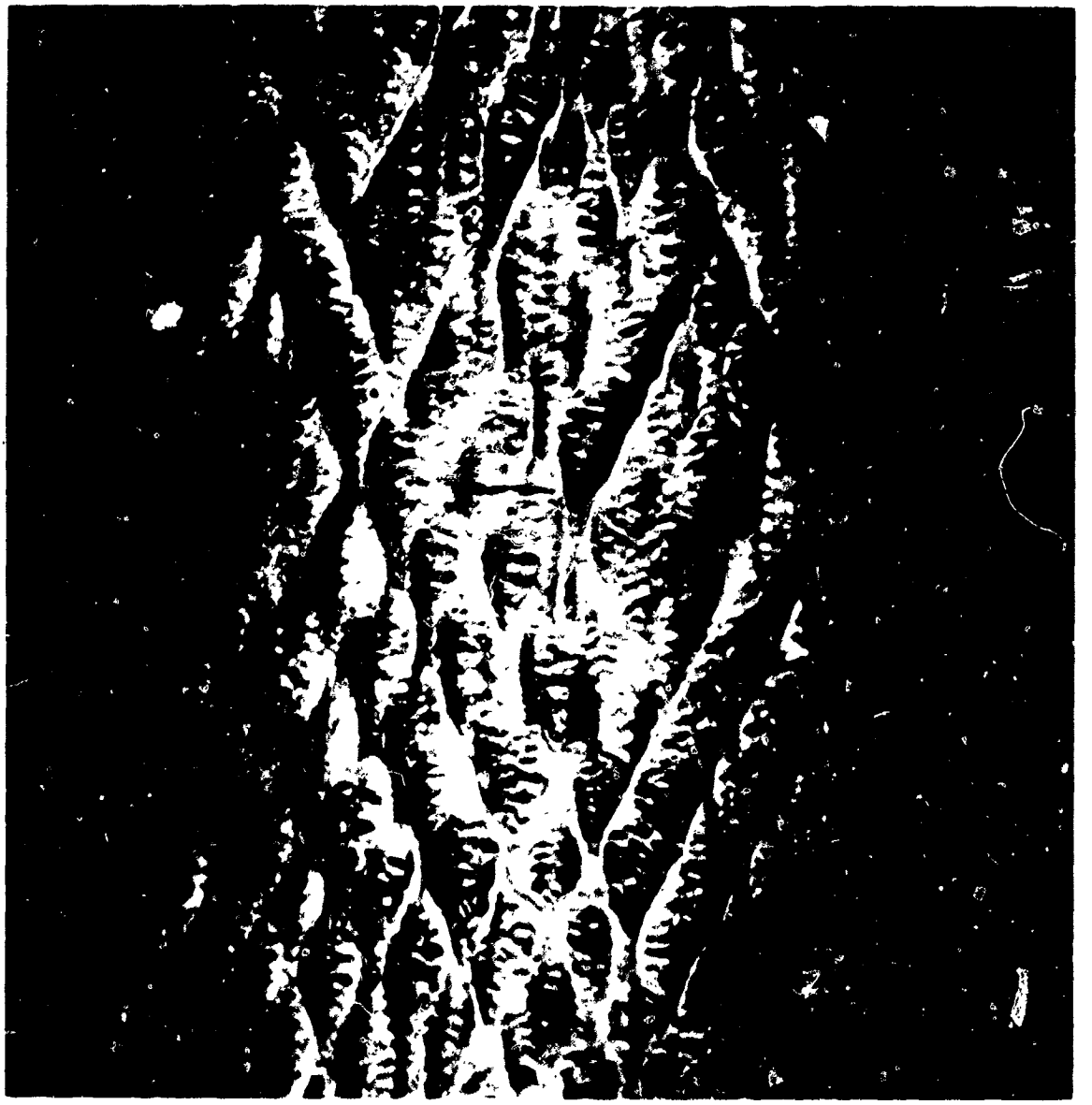

Fig. 1. Example of cross-hatching (Ref. 10).

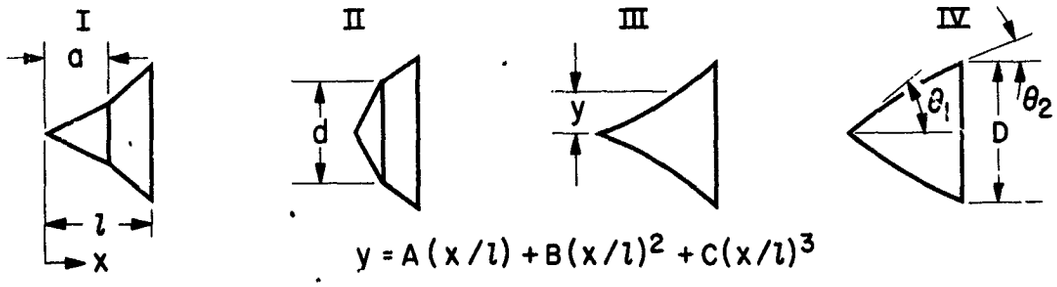

$$y = A(x/l) + B(x/l)^2 + C(x/l)^3$$

MODEL No.	CLASS	θ_1, deg	θ_2, deg	D, cm	d, cm	l, cm	a, cm	P_s**, atm	T_s‡, °K	TEST TIME, sec	A, cm	B, cm	C, cm
1	I	25	40	21.23	9.921	17.38	10.63	120	778	19	—	—	—
2	I	30	45	19.32	10.16	13.38	8.796	118	742	28	—	—	—
3	III	25	40	21.23	—	17.38	—	118	773	21	8.1033	1.0637	1.4502
3*	III	25	40	21.23	—	17.38	—	121	1075	35	8.1033	1.0637	1.4502
4	II	50	35	20.32	11.68	11.07	4.892	122	776	17	—	—	—
4*	II	50	35	20.32	11.68	11.07	4.892	116	764	52	—	—	—
5	IV	50	35	20.32	—	11.07	—	118	761	29	13.195	-3.6627	0.6276
6	IV	40	25	23.50	—	18.97	—	110	743	71	15.918	-5.4400	1.2693
7	III	30	45	19.32	—	13.38	—	117	763	40	7.7254	0.15502	1.7818
8	II	40	25	23.50	13.06	18.97	7.777	114	746	51	—	—	—

*SECOND TEST
**NOMINAL WIND TUNNEL STAGNATION PRESSURE
‡STAGNATION TEMPERATURE

Fig. 2. Model dimensions and test conditions.

(a) Model No. 1.

(b) Model No. 2.

Fig. 3. Replicas of ablated models.

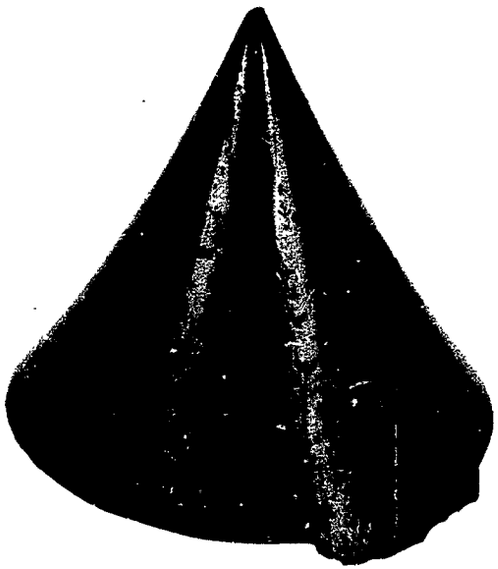

(c) Model No. 3 (first test).

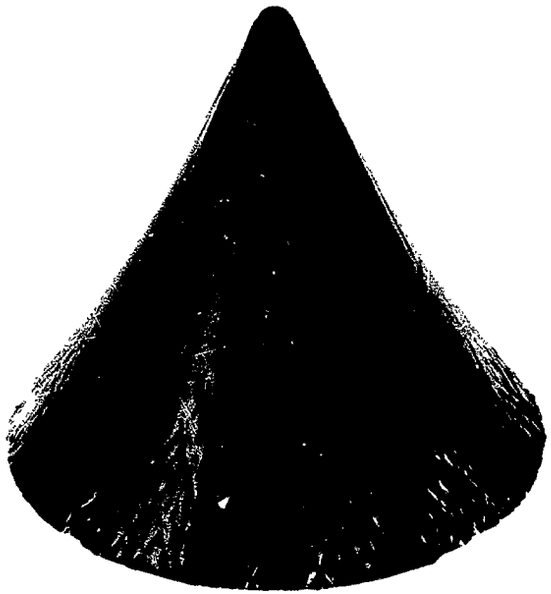

(d) Model No. 3 (second test).

Fig. 3. Continued.

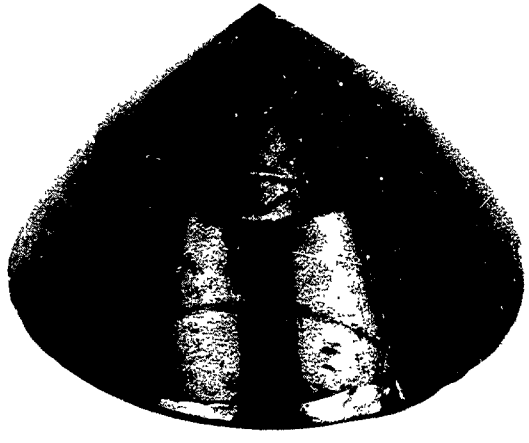

(e) Model No. 4 (first test).

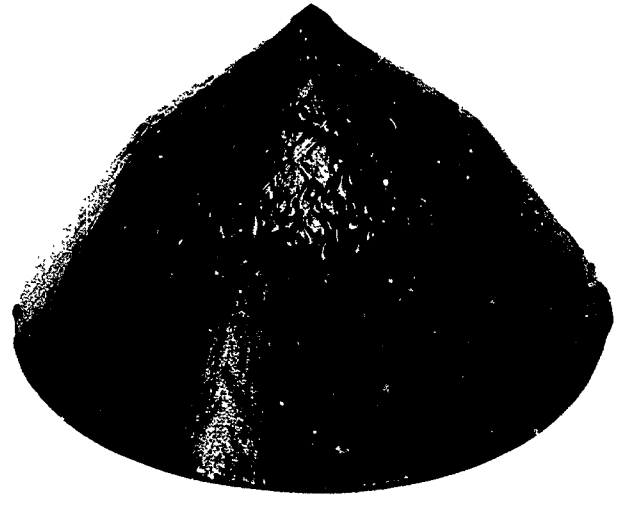

(f) Model No. 4 (second test).

Fig. 3. Continued.

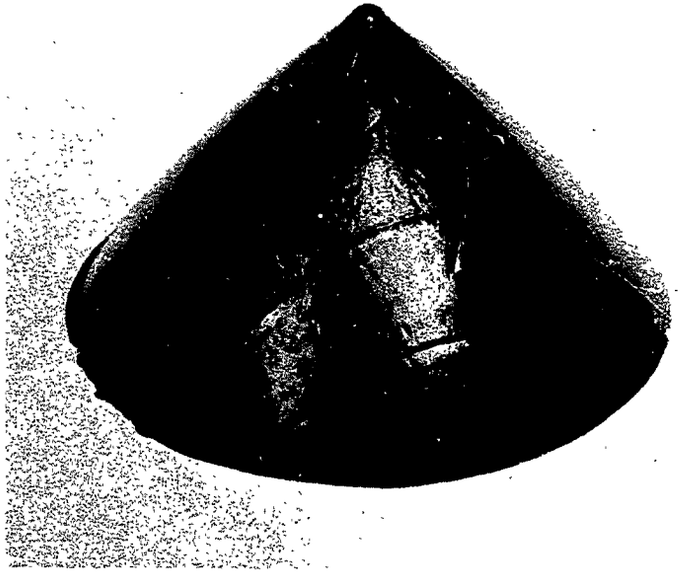

(g) Model No. 5.

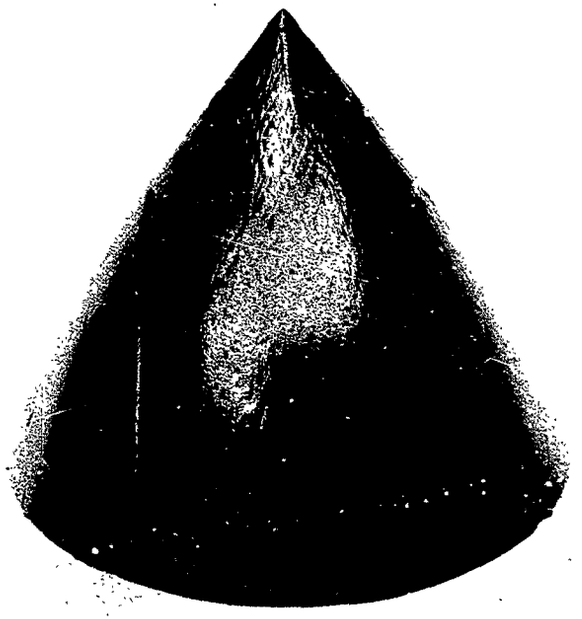

(h) Model No. 6.

Fig. 3. Continued.

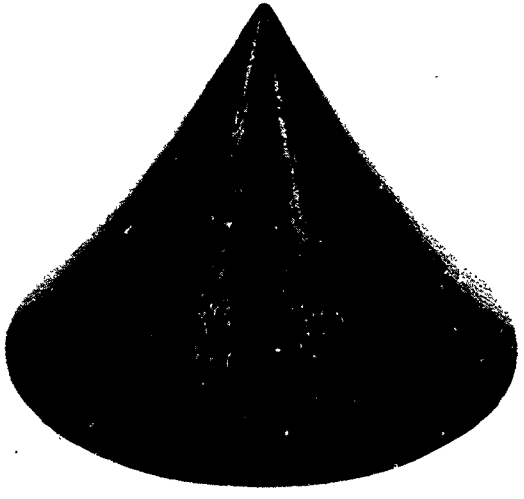

(i) Model No. 7.

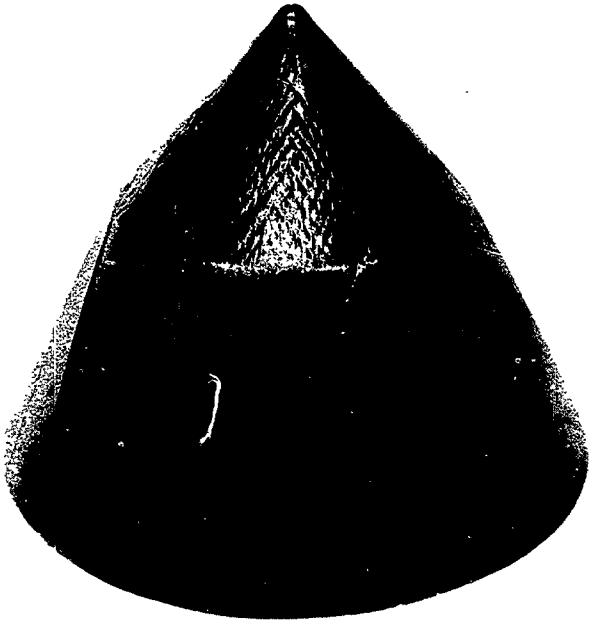

(j) Model No. 8.

Fig. 3. Concluded.

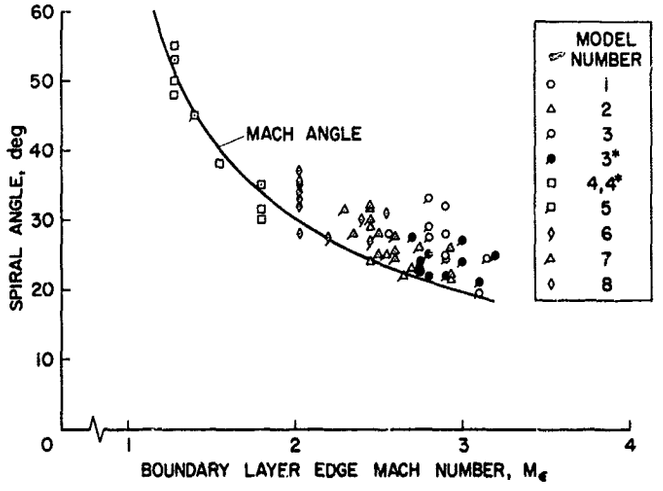

Fig. 4.
Variation of crosshatch spiral angle with boundary-layer-edge Mach number.

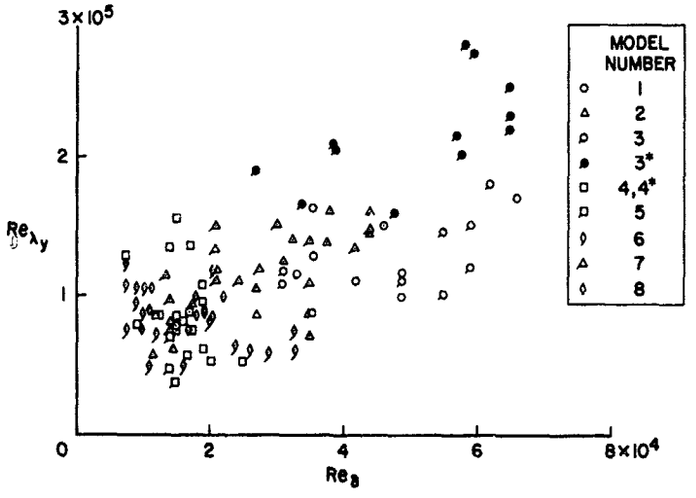

Fig. 5.
Lateral spacing Reynolds number versus boundary-layer thickness Reynolds number.

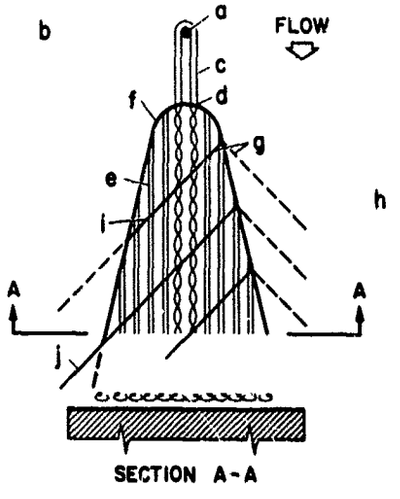

Fig. 6. Diagram of postulated flow model.

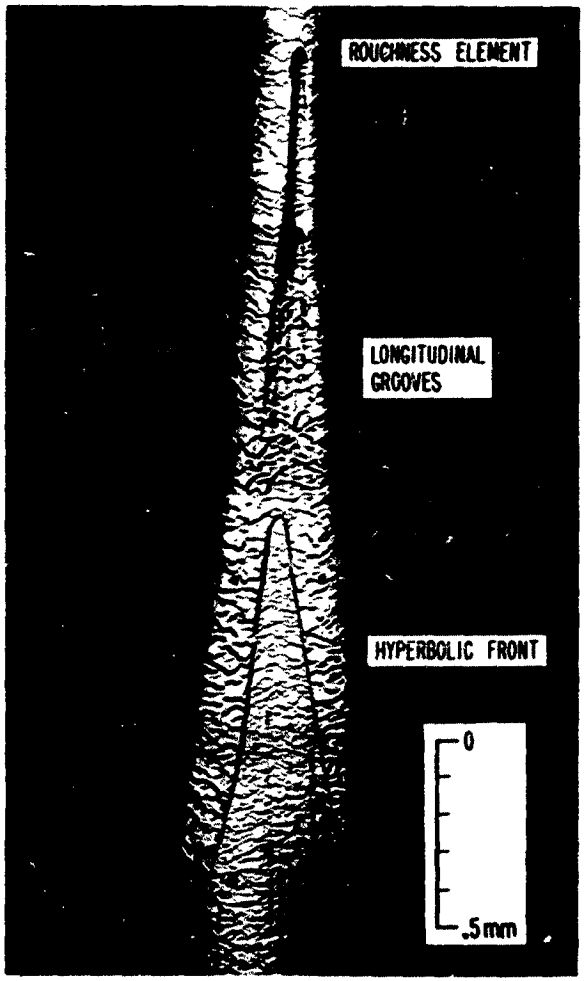

(a) Ballistic-range model (Ref. 9).

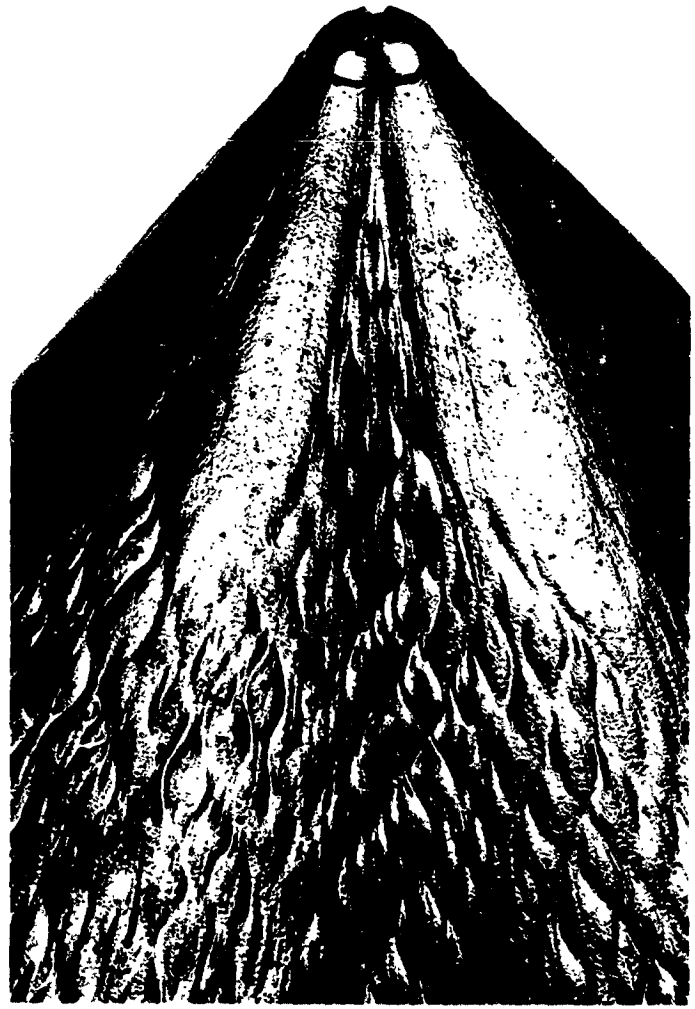

(b) Nose region of Model No. 8.

Fig. 7. Turbulent wedges.

PAPER 7

This paper has been cancelled
by mutual agreement

REYNOLDS AND MACH NUMBER SIMULATION OF APOLLO AND GEMINI RE-ENTRY AND COMPARISON WITH FLIGHT

By

B. J. Griffith and D. E. Boylan
ARO, Inc., Arnold Air Force Station, Tennessee

SUMMARY

A comprehensive investigation in the AEDC-VKF wind tunnels was conducted on the Apollo 011 and Gemini 3 spacecraft configurations in order to resolve several anomalies between preflight predictions and flight data. Attention was focused on simulating the actual Apollo Command Module (011) and Gemini spacecraft (GT3) "as flown" in model construction over a Mach number range of 3 to 20.

The investigation indicated that the influence of the ablator (heat shield) geometry of the Apollo Command Module causes a significant change in trim angle of attack and resulting decrease in available lift-to-drag ratio. In addition, a very strong viscous influence exists in the initial portion of re-entry for both the Apollo and Gemini spacecrafts. Also, the Mach number influence extends up to about Mach 14 which is substantially higher than previous blunt body investigations have indicated. Comparisons of the AEDC wind tunnel data with existing flight data are made and generally excellent agreement exists.